Assessment of the performance of river replenishment of sediment applied to a non-erodible channel by means of numerical modeling

C. Juez[a,1,*], E. Battisacco[a], A. J. Schleiss[a], M. J. Franca[a]

[a]*École Polytechnique Fédérale de Lausanne (EPFL), Laboratoire de Constructions Hydrauliques (LCH), Lausanne, Switzerland*

Abstract

The artificial replenishment of sediment is a method used to solve the lack of sediment continuum in the downstream reach of dams. The understanding of the impact of this technique on flow and bed morphology in rivers is a challenging. Furthermore it is an up-to-date topic since the restoration of sediment dynamics highly impacts on biodiversity and quality of the water courses. The potential of numerical schemes as a forecasting tool for the decision-making processes of these replenishment procedures is still poorly understood. In this work, 2D shallow water equations in combination with the Exner equation are solved by means of an augmented Riemann solver. Computational outcomes are compared with experimental data obtained from several replenishment configurations studied in the laboratory. The classical friction approach considered for mimicking the bed channel roughness has been modified for taking into account the effect of the replenishment, which plays an important role on the temporal evolution of the channel bed roughness. Results point out the promising prediction capacity of the numerical solver, which can be used to evaluate currently applied or to forecast the behavior of planned replenishments.

Keywords: 2D Shallow water, sediment replenishment, bed-load transport, dam impact, bed-shear stress, sediment management

*Corresponding Author

Email address: carmelo.juez@epfl.ch (C. Juez)

[1]Tlf.: (+41)2169 36326

Manuscript accepted in *Advances in Water Resources* *November 17, 2015*

1. Introduction

In the downstream reaches of dams the sediment continuum is altered by the dam presence. Without sediment release structures, a dam traps the sediments in the upstream reservoir, especially during floods, creating an obstacle to the natural sediment transport [1, 2, 3]. Due to the absence of sediment transport, many negative changes may occur along rivers on both the morphological and ecological aspects. The main morphological effects are related to tendency to riverbed incision, generation of an armored layer and coarsening of the bed, together with bank instability and changes in channel width. These changes negatively affect also the ecosystem along the river, inducing a loss in the aquatic and riparian habitats with consequences on the water quality [4, 5, 6, 7]. The above-mentioned outcomes limit the possibilities for fish spawning and survival.

In the last decades, the replenishment of sediment (also called gravel augmentation) technique has been applied in order to supply sediments lacking in the downstream reaches. The artificial addition of sediments into the rivers has been used since the 80' with the main purpose to recreate a natural sediment transport [8]. More recently, it was stated in [9, 10] that the added material for replenishment purposes should be smaller than the existing bed material in order to favor the fine sediment availability for the spawning habitats and to enhance bed elevation variations. Conversely, field experiments, carried out in the United States and in several Japanese and European rivers, as well as laboratory investigations have permitted to improve the knowledge on the complex geomorphological processes occurring in rivers subjected to the replenishment of sediment [11, 12]. Nowadays, the replenishment of sediment is more often applied in rivers for geomorphic purposes, using a specific grain size, to maintain or even increase the morphology variety including bed forms in a channel [13, 14, 12]. Extension and duration of the morphological bed changes obtained by gravel augmentation are very important in determining the effectiveness of the method [15]. During the last years, several laboratory experiments were performed permitting to assess the general erosion process of deposits [7], the evolution of sediment waves [16, 17, 15] and the influence of added sediment supply on river bed morphology [18, 10, 19, 20]. In particular, the erosion process of sediment deposits is presented by the laboratory results from [7]. Here, the erosion mechanism is described as a combination of lateral erosion on the sediment deposit toe by hydraulics forces, and the subsequent mass failure

by gravitational mechanism due to the over steepening of the banks. Field observations downstream the Murou dam confirm these laboratory findings [7]. After collapsing, the eroded mass of the replenishment is transported further downstream. Translation and dispersion are the two main transport types occurring for sediment augmentation [15, 17]. In an ideal performed replenishment, as stated in [15], sediments would firstly be transported by translation to the downstream target reach and, then they should shift progressively to a dispersion transport mechanism.

Beside the field and the laboratory experiments, numerical morphodynamic models have been developed as a support of making-decisions about the replenishment technique. [21] remarked that their numerical tool was not reliable in predicting the magnitudes in bed elevation changes and failed to reproduce the riffle-pool-pattern observed in field experiments with sediment replenishment. In [22] the incapacity in anticipating the bed load transport in gravel bed rivers by any of sediment transport formulas was stated. Hence, the gap of knowledge about the existing link between sediment supply and channel bed morphology has still to be fulfilled [16, 19]. More detailed studies are required on the influencing factors affecting the success of gravel augmentation projects, since the conceptional design of many of the restoration projects are still designed based only on past experiences [5, 7, 15]. Above all, the role played by the discharge, the necessary amount of sediments and the mechanism of sediment propagation through the channel are core to better understand [7, 19]. Since in-situ monitoring campaigns are difficult to carry out and considering that the laboratory experiments cannot fulfill all the non-yet investigated domain, the implementation of numerical tools arises as a helpful approach for better understanding the morphological consequences due to a sediment replenishment.

In this work the 2D depth-averaged mathematical model was considered since this set of equations is widely accepted in the study of river configurations and the number of equations and closure relations is limited. The morphodynamic evolution of the replenishment material is computed by means of the Exner equation. The spatial and temporal evolution of the hydrodynamic and morphodynamic models must be solved through a synchronous treatment, [23], since there is a strong interaction between the flow and the replenishment material. There are several numerical techniques present in literature for solving this set of equations: Finite Volumes (FV) [24, 25, 26, 27], Finite Elements (FE) [28] and Finite Differences (FD) [29]. Based on a explicit Finite Volume strategy described in [30] an efficient and self-stable nu-

merical scheme was validated successfully against experimental data. Hence, this numerical tool will be used for studying the hydro-morphodynamic behavior of the replenishment process when dealing with different configurations.

The remainder of the paper is structured as follows: first the methodology to obtain the experimental data is described. Then the next section is devoted to briefly outline the mathematical model and numerical scheme considered. The following section presents the results obtained with this study and their prior discussion. Finally, the conclusions of the work are summarized.

2. Experimental Methodology

Series of laboratory experiments to test different replenishment of sediment configurations were performed at the Laboratory of Hydraulic Constructions (LCH) at École Polytechnique Fédérale de Lausanne (EPFL), in Switzerland. The tests are performed in a 15 m long channel with a bed width of 0.4 m. The bank slope is 2:3 (height:length) and the longitudinal slope 0.015, Figure 1. The length of the replenishment volumes, L, is equal to 0.64 m. The discharge is controlled by a pump system. The water flows from an upper stilling basin throughout the channel reaching the outlet basin downstream. The discharge is indirectly determined by the imposed replenishment submergence condition. The replenishment height is kept constant and, in the herein presented experiments, the discharge corresponds to a completely submergence condition of the volume (volume height=water depth) equal to 19 l/s on model. The laboratory model has an approximate 1:10 scale factor considering the geometric characteristics of a typical alpine river. In Figure 2, the grain size distributions for the channel bed and for the replenishment material are displayed. The bed grain size distribution, used for creating the fixed bed and the banks, is representative of a typical alpine river. The replenishment volumes are composed of a finer grain distribution which dimension varying from 3 to 8 mm. The ecological needs for spawning grounds, scaled to laboratory scale, were considered in this grain choice [9, 10]. Each test lasts three hours. In a preliminary analysis on the evolution of the morphological bed forms demonstrated that, with this flow condition, a certain morphological equilibrium is reached in two hours, [31].

The influence of different amounts of replenishment together with four different geometrical configurations were investigated. Specifically: single volume (configuration 1), double volumes aligned (configuration 2), parallel

(configuration 3) and alternated (configuration 4) configurations are proposed, Figure 3. While in configuration 3 the volumes are symmetrically placed on the banks, in configuration 4 the two blocks on one bank are switched downstream by a distance equal to half the replenishment length. In each test the same block volume dimensions are maintained, thus the configurations 2, 3 and 4, with multiple volumes, have respectively two and four times the amount of gravel of configuration 1. Data analysis is performed by means of photos taken at different time steps during the tests. A camera is installed on a carriage moving along the downstream and the traversal directions, and the photos are taken each 0.5 m along the channel and then merged together forming a panoramic view. In order to facilitate the analysis and the detection of the transport motion, the grains composing the replenishment were painted in red.

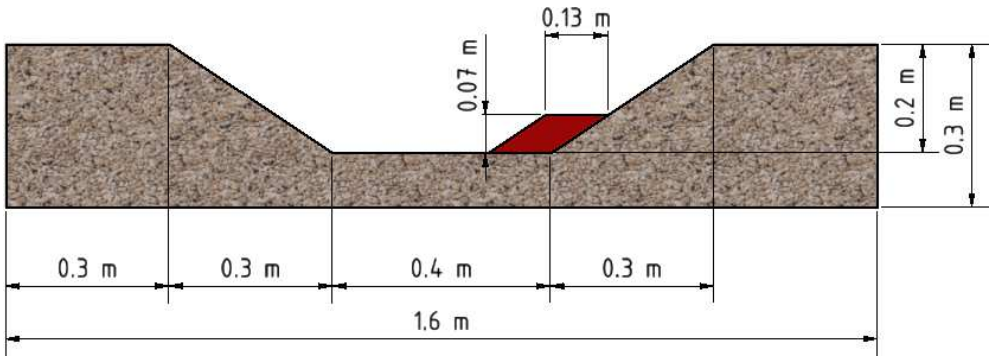

Figure 1: Cross section view of the channel with one replenishment reproduced at the bank

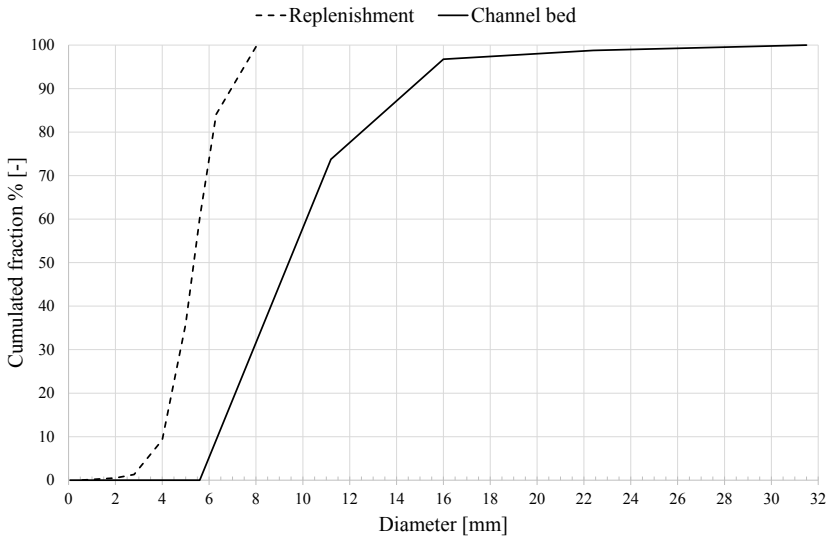

Figure 2: Grain size distribution for channel bed and replenishment material

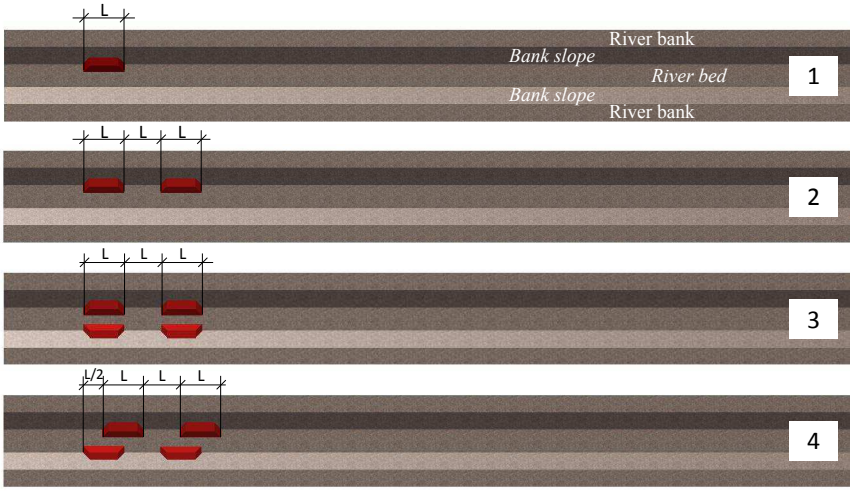

Figure 3: Volumes configurations 1, 2, 3 and 4 for the replenishment

3. Simulation Methodology

3.1. Flow simulation

The mathematical model is built by 2D shallow water equations, SWE, and the Exner equation. The SWE are derived from the Navier-Stokes equations by integrating the continuity and momentum equations over depth, [32]. The resulting 2D system of equations is written in the conservative form as follows

$$\frac{\partial \mathbf{U}}{\partial t} + \frac{\partial \mathbf{F}(\mathbf{U})}{\partial x} + \frac{\partial \mathbf{G}(\mathbf{U})}{\partial y} = \mathbf{T}_\tau + \mathbf{T}_b \tag{1}$$

where

$$\mathbf{U} = (h, hu, hv)^T \tag{2}$$

are the conserved variables with h representing water depth in the vertical coordinate and (u, v) the depth averaged components of the velocity field. The flux terms are expressed as

$$\begin{aligned} \mathbf{F} &= \left(hu, hu^2 + \frac{1}{2}gh^2, huv\right)^T \\ \mathbf{G} &= \left(hv, huv, hv^2 + \frac{1}{2}gh^2\right)^T \end{aligned} \tag{3}$$

being g the gravity acceleration.

The source terms $\mathbf{T}_\tau$ and $\mathbf{T}_b$ collect, respectively, the information about the friction exerted over the bed, evaluated through the 2D Manning's law, and the gravity forces written by means of the bed slopes,

$$\mathbf{T}_\tau = \left(0, -gh\frac{n^2 u\sqrt{u^2+v^2}}{h^{4/3}}, -gh\frac{n^2 v\sqrt{u^2+v^2}}{h^{4/3}}\right)^T \qquad \mathbf{T}_b = \left(0,\ -gh\frac{\partial z}{\partial x}, -gh\frac{\partial z}{\partial y}\right)^T \tag{4}$$

with n the Manning's parameter and z the bed elevation.

On the other hand, the bed evolution is modeled through the Exner equation, which is a continuity equation where the bed level is modified by

the solid fluxes which cross the control volume. The 2D Exner equation for bedload is written as follows,

$$\frac{\partial z}{\partial t} + \xi \frac{\partial q_{s,x}}{\partial x} + \xi \frac{\partial q_{s,y}}{\partial y} = 0 \tag{5}$$

where $\xi = \frac{1}{1-p}$, being p the material porosity and $q_{s,x}$, $q_{s,y}$ the solid fluxes which are computed as a function of excess bed shear stress with respect to the critical value. This bedload transport is often written through the following dimensionless parameter,

$$\Phi = \frac{|\mathbf{q}_s|}{\sqrt{g(s-1)d_m^3}} \tag{6}$$

where $s = \rho_p/\rho_w$ is the ratio between solid material (ρ_p) and water (ρ_w) densities, and d_m is the median diameter of the transported sediments. According to the numerical assessment performed in [33], the Smart formula is chosen for computing the bedload discharge, which in dimensionless form is written as follows

$$\Phi = 4 \ (d_{90}/d_{30})^{0.2} \ Fr \ S^{0.1}\theta^{1/2}(\theta - \theta_c^S) \tag{7}$$

where the term S is the bed slope which is evaluated as in [33] for distinguishing between in favor and adverse sloping beds, d_{90} and d_{30} are the characteristics diameters of the sample, Fr is the Froude number, θ is the dimensionless shear stress and θ_c^S is the critical shear stress according to [34].

The computational method considered for solving the equations is fully explained in [30] where the computational domain is split in fixed computational cells. Then, the Gauss theorem is applied to each volume cell for computing the solid and liquid fluxes which cross the edge of each cell. These fluxes are derived from an approximate Riemann Problem. Then, the conserved variables are updated in time and space by means of an upwind technique considering a first order approach. The stability criteria is controlled thanks to an augmented CFL condition proposed in [30].

3.2. Friction law

One of the key parameters which governs the dynamics of the sediment replenishment is the roughness of the water-worked bed. This roughness is influenced by bed mobility which has an impact on the mean longitudinal velocity and on the bed shear stress, [35, 36]. The rheological law which is

considered in this work for modeling the friction is the Manning's law, [37]. This law is based on a power-law velocity model where the friction over the bed is written as the product of a friction parameter and the square of the depth-averaged velocity, equation (4). This Manning friction parameter may be related with the grain size by means of the Strickler formula for armored channels, [38]

$$n = \frac{1}{26} d_{90}^{1/6} \tag{8}$$

Furthermore, the addition of replenishment material to the channel causes secondary effects. Due to the finer nature of the sediments of the replenishment, the initially coarser non-erodible channel suffers a change in the surface roughness, i.e. the sediments coming from the replenishment build a new layer over which the water column exerts a new friction value. In order to take into account this important characteristic, the Manning parameter is continuously updated during the simulation as follows

$$n = \begin{cases} \frac{1}{26} \left(d_{90}^{C}\right)^{1/6} & if \quad DD \leq d_{90}^{C} + d_{90}^{R} \\ \frac{1}{26} \left(d_{90}^{R}\right)^{1/6} & if \quad DD > d_{90}^{C} + d_{90}^{R} \end{cases} \tag{9}$$

where d_{90}^{C} and the d_{90}^{R} are the d_{90} for the non-erodible channel and the replenishment material respectively, and DD is the deposition depth of the added material for replenishment purposes.

This effect of bed fining has been confirmed in gravel-bed rivers [39, 40] and in sand-bed rivers [41, 42, 43]. For these situations, this phenomenon is a consequence of dune sorting, hydraulic structures, overbank deposition and river bifurcation. In this work, the bed fining is a consequence of the finer material of the replenishment.

4. Results & Discussion

4.1. Description of the experimental results

The 2D temporal evolution of the covered surface occupied by the replenishment material during the experiment is displayed in Figures 4, 5, 6, 7 (top views). Visual observations during the experiment show that the erosion of the blocks of replenishment occurs as a combination of fluvial erosion at the deposits toe and mass failure of the above placed sediment due to over-steepening. The collapsed mass is then further eroded and transported

downstream by the flow. Furthermore, in configurations 2, 3 and 4 the most upstream volumes of added material are less eroded than the following downstream replenishments. For configurations with parallel volumes, 3 and 4, the deposition of the eroded replenishments occurs further downstream. The pattern of depositions in the downstream channel varies among configurations.

Considering each configuration, in configuration 1 most of the material is preserved in the original location. The small amount of eroded sediments is settled in the vicinity of the channel wall. Configuration 2 (Figure 5) with two blocks in the same side leads to similar results. The material eroded from the replenishment located upstream is not able to affect the second block. Configuration 3 (Figure 6) is a step further in morphology complexity. Being the replenishment parallel aligned on the banks, in the first phases of the experience, they create a fix obstacle for the flow. In this case, the flow is forced to propagate between the blocks, i.e., in a narrower section compared to the upstream section. Thus, the flow velocity increases and the erosion rates increase as well. The above-mentioned behavior lasts until the upstream replenishment is eroded; then the flow velocity decreases together with the erosion rate, which reaches an equilibrium state. Compared with the results from configurations 1 and 2, in this case the sediments are more dispersed and more clustered depositions appear along the channel. Finally, the same behavior is observed for configuration 4 (Figure 7) which, in comparison with configuration 3 (Figure 6), shows the relevant influence of the geometrical block placement. The non-complete alignment of the replenishment upstream slows down the erosion rate and enhances the creation of a bed form pattern downstream.

4.2. Comparison of the temporal evolution of the deposition evolution

Numerical results are herein compared to the experimental data obtained in the laboratory for the four replenishment configurations explained in Section 2.

The computational domain has been discretized using a non uniform triangular mesh of 32000 cells, locally refined along the center area of the channel. The smallest triangle area is approximately 0.0006 m^2. At the inflow cross-section, a constant discharge equal to 19 l/s is imposed and at the outflow a free boundary condition is considered.

Figures 4, 5, 6, 7 (bottom views) show the temporal evolution of the computed and experimental results in terms of deposition downstream the re-

plenishment. The numerical results comprise 3D contours views whereas the experimental data contains 2D information obtained from the photo survey of the tests made along the time. For configuration 1, Figure 4, the material spreading covers up to 2 m downstream the block. The general tendency is well tracked by the numerical scheme. For the second configuration, Figure 5, the maximum run-out (i.e. spreading) of the material is also limited and it advances 2.5 m considering the second volume of sediment. Nevertheless, the computational results are able to reproduce the phenomenon. Moreover, as visible on the experimental results, the erosion rate for both configuration 1 and 2 is not complete since the completely submerging condition in those configurations is not enough for mobilizing the replenishment. The numerical model predicts well the behavior, achieving a maximum deposit height, at the end of the simulation of around 0.04 m.

For configuration 3 (Figure 6) the computational results predict the strong mobilization of the material, which is washed away from its original location. The maximum mobilization of the material observed in the experiments, 12.5 m, is almost reached with the numerical scheme. For configuration 4 (Figure 7), the spreading of the material is again relevant, overtaking the channel length of 12 m. Newly, the constraint effect of the flow produced by the volumes leads to stronger erosion processes. The numerical scheme predicts successfully the maximum run-out. It is also able to reproduce the movement of the material of one of the downstream blocks which is almost completely removed and settled downstream due to the effect of the water. Conversely, although the maximum spreading and general trend is computationally well achieved, the geomorphological patterns that exhibit configurations 3 and 4 are not accurately tracked. Indeed, the numerical scheme is not able to reproduce the free replenishment material areas followed by dense spatially-occupied areas.

Additionally, the effect of the roughness evolution of the channel due to the replenishment is herein further analyzed. For this purpose, Figure 8 displays the stage at time t=30 min for the configuration 3 with a constant Manning parameter (i.e. considering only the roughness arising from the bottom material) and with a Manning parameter related with the deposition depth (i.e. assuming a shift between the roughness of the bottom and the roughness of the replenishment material). As it is observed, the overall surface level of the replenishment is completely different between them and also with the experimental data provided in Figure 6. An important mismatch of a physically based behavior is observed when the Manning parameter is kept

constant for all the computational domain. Therefore, the dynamic adaptation of the Manning parameter plays a key role and it has to be retained in the model. Nevertheless, it is worth noting that the larger amount of replenishment material is spread over the channel, the more relevant becomes this approach for computing the friction.

4.3. Parameter analysis

An important parameter when dealing with replenishment techniques is the occupational ratio (OR). This parameter is based on a 2D analysis and it shows the fraction of area that is covered by the replenishment material:

$$OR = \frac{A_R}{A_T} \tag{10}$$

where A_R is the area which is occupied by the replenishment material and A_T is the total area under analysis. This parameter has been computed for traversal slices of the channel with 0.1 m length. The OR aims at identifying the level of material aggregation on the channel along the longitudinal direction. For an adequate sediment replenishment process a dispersion behavior of the added material is required to achieve the most common goals to improve rivers ecology, such as fining bed grain size and enhanced bed elevation variations in order to improve rivers ecology. Hence, the OR quantifies the dispersion of the material of the replenishment along the channel.

Figure 9 shows the temporal evolution of the computational and experimental occupational ratio for each configuration tested in this work. The initial OR of the deposits of sediment are quickly increased as a consequence of the sediment transport. Sediments are washed out by the flow and the particles are spread along the channel until reaching an equilibrium stage. The time analysis of the OR shows that the position of the peaks is approximately constant in the channel. The general tendency is well reproduced by the numerical scheme, where the maximum run-out of the material is achieved for the four configurations. The values of the OR are similar over the replenishment blocks. The main differences appear in the third and fourth configurations downstream the blocks location: sediment patterns are observed in terms of a sequence of peaks of occupational ratio. In particular for configuration 4, a clear bed form pattern (transversal bars) is observed on the channel bed at the end of the experiment. The same behavior is not noticeable in the results performed by the numerical simulation. Generally, the numerical model tends to underestimated the ratio of OR. Nevertheless, the

difference-ratio is constant between the analyzed configurations, confirming the reliability of the numerical method.

Travel distance (TD) of the center of mass is another important parameter which allows to verify the geomorphological response of the channel bed to gravel augmentation under given geometric and hydrodynamic conditions. The higher the TD value is, the bigger the impact of the replenishment is in the downstream direction. Furthermore, the analysis of the TD over time allows to estimate the propagation velocity of the sediment transport. The slope in the temporal evolution of transport distance can be seen as a transport velocity, where steep slopes indicate a fast movement. Furthermore, the position of the center of mass can be estimated for the entire deposition region observed or partially for several percentiles. Hence, TD_x is the position where the $x\%$ of the covered surface is located downstream. Figure 10 displays the travel distance for several percentiles of the covered surface for the computational results and the experimental data. Transport velocity for TD_{75} and TD_{95} are higher than of TD_{25} and TD_{25}. Each percentile travels quicker during the first minutes; afterward, the transport velocity tends to slow down until a equilibrium stage is reached. Moreover, for configurations 3 and 4, the percentiles of the TD reach the downstream part of the channel faster due to the effect of the bed fining. Regarding the numerical-experimental comparison, there is an accurate agreement between both results, although the experimental travel distance is always above the computational prediction. This is justified by the fact that the maximum run-out with the laboratory data is slightly larger than the one obtained with the numerical tool.

The sediment patterns in terms of occupability ratio found in configuration 3 and 4, as it has been mentioned before, are not accurately reproduced by the numerical scheme, Figure 9. This can be justified by the fact that some areas of those patterns, visible in the photo survey of the experiment, are composed by a few layers of material (1-2 grains), where the friction term acting on the sediment is not only governed by a basal force, but also by the local collision forces among particles. With the present model, based on a continuum approach, these features are not included. Further, the bed roughness of the channel exhibit a chaotic nature, in the sense that although a characteristic d_{90} can be estimated from the numerical simulations, the spatial distribution of such sample is random. This fact can alter significantly the patterns since they are built with 1-2 grains. However, the areas with high occupation of particles are better modeled by the numerical scheme and this is justified by the good fit observed in the occupational ratio and in the

travel distance, Figures 9 and 10.

4.4. Bed shear stress

Regardless the configuration, the global roughness of the downstream bed is reduced by the finer replenishment. Thus an increase of the bed shear stress and of the transport capacity are observed. This result is in agreement with the reaction of steep mountain gravel streams to a first sediment pulse input, observed by [44] and with recent morphodynamic modeling, where a fining of the bed surface due to increased sediment supply is predicted [45]. Furthermore, the decrease in roughness is in good correspondence with OR, as for highest OR also the largest bed fining is observed, Figure 9.

For the reasons mentioned above, the estimation of the bed shear stress is challenging in both field and laboratory conditions, especially with mobile sediments. At the same time, knowing the value of the bed shear stress is crucial for evaluating the performance of occupability ratio and travel distance. In this context, the numerical tool becomes helpful in forecasting the results for different replenishment proposals since by means of equation (9) the friction coefficient is continuously updated for each cell of the domain. Figure 11 displays the temporal evolution of the bed shear stress for configuration 4. Zones having alternating higher and lower bed shear stress are observed. Through numerical modeling and taking into account the replenishment purpose (rehabilitation of the sediment continuum), it is possible to determine the erosion, transport and aggradation of the sediment which is fed in the channel. Hence, it will be known: (i) where to place the replenishment, (ii) when to do it, (iii) which is the more suitable configuration of blocks and (iv) if it is required to repeat the replenishment for an effective final result.

Time t = 10 min .

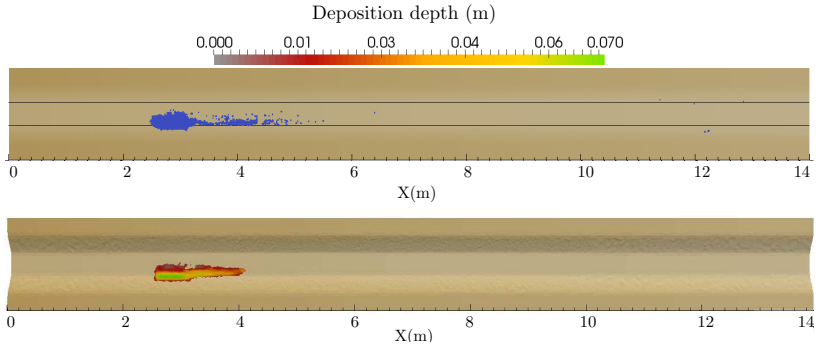

Time t = 30 min .

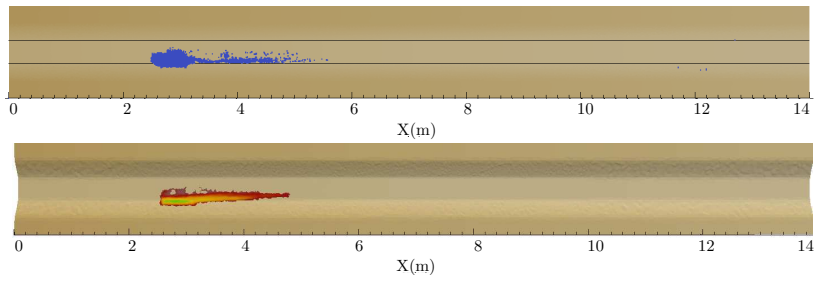

Time t = 120 min .

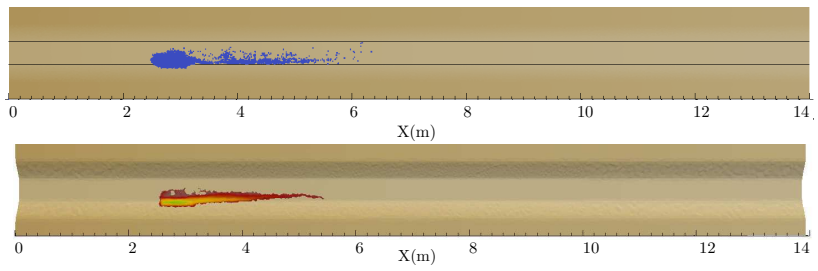

Figure 4: 2D experimental data of the covered surface (top views) and 3D computed contour views simulated numerically (bottom views) for the deposition depth along the non-erodible channel at times t= 10, 30 and 120 *min* for configuration 1

Time t = 10 min .

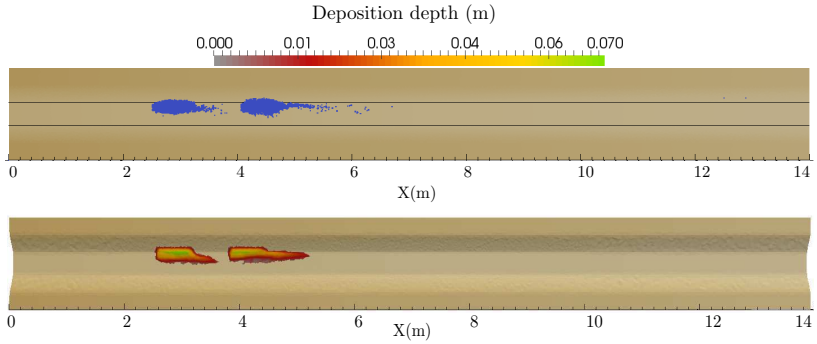

Time t = 30 min .

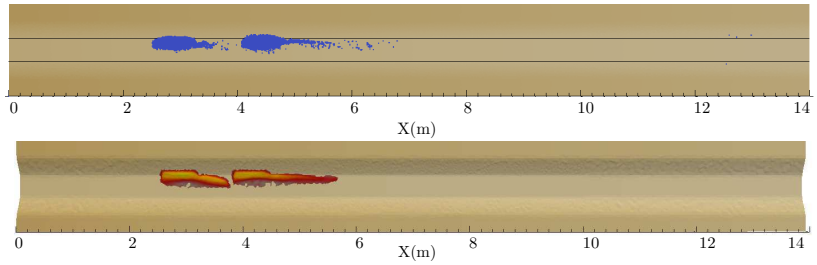

Time t = 120 min .

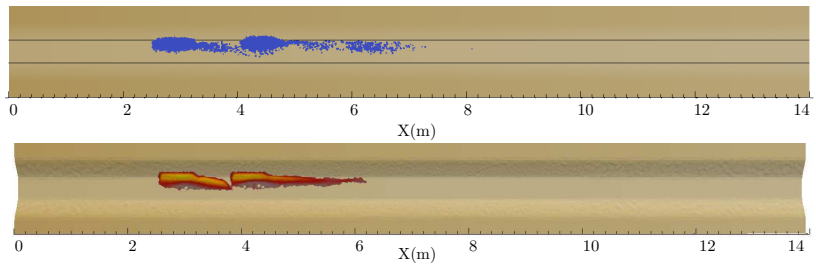

Figure 5: 2D experimental data of the covered surface (top views) and 3D computed contour views simulated numerically (bottom views) for the deposition depth along the non-erodible channel at times t= 10, 30 and 120 *min* for configuration 2

Time t = 10 min .

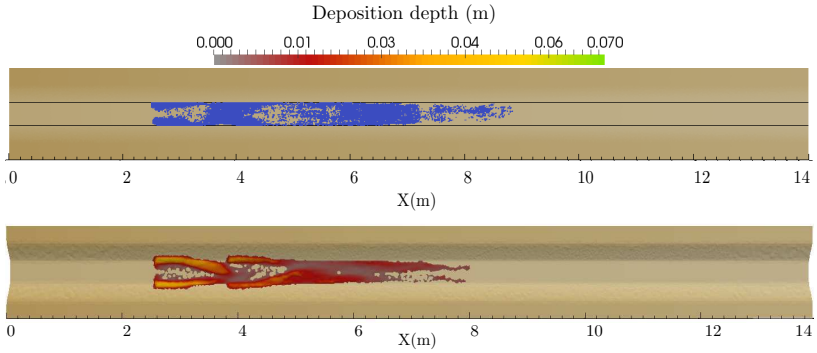

Time t = 30 min .

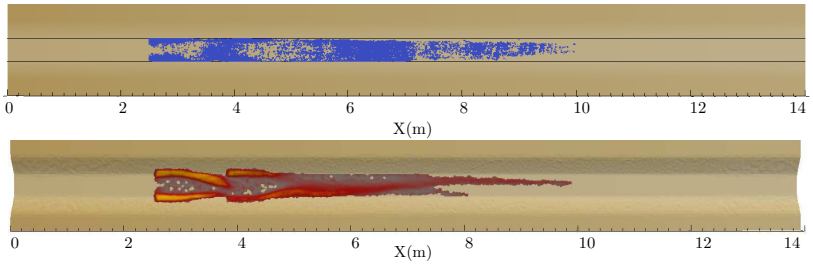

Time t = 120 min .

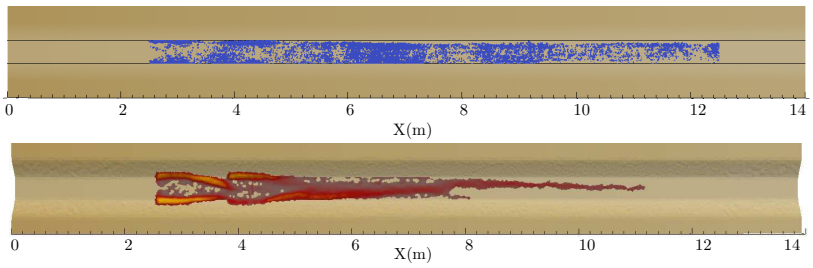

Figure 6: 2D experimental data of the covered surface (top views) and 3D computed contour views simulated numerically (bottom views) for the deposition depth along the non-erodible channel at times t= 10, 30 and 120 *min* for configuration 3

Time t = 10 min .

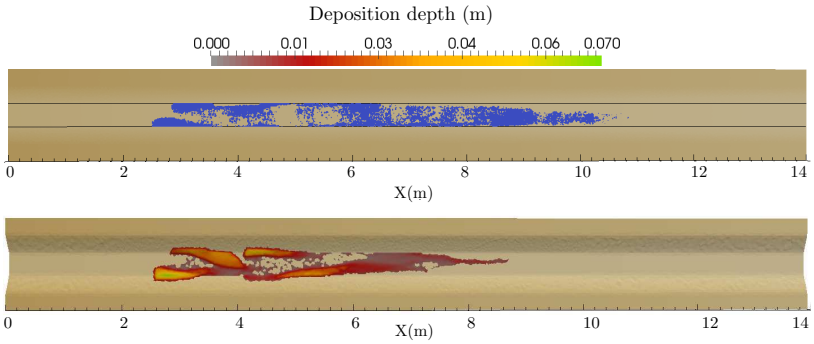

Time t = 30 min .

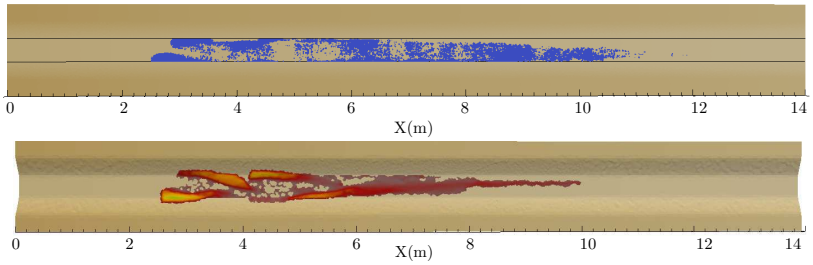

Time t = 120 min .

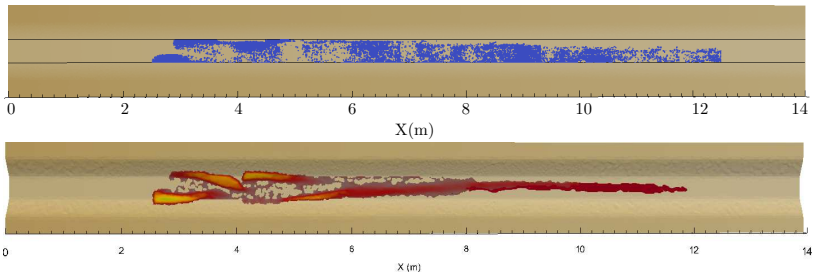

Figure 7: 2D experimental data of the covered surface (top views) and 3D computed contour views simulated numerically (bottom views) for the deposition depth along the non-erodible channel at times t= 10, 30 and 120 *min* for configuration 4

Configuration 3 .

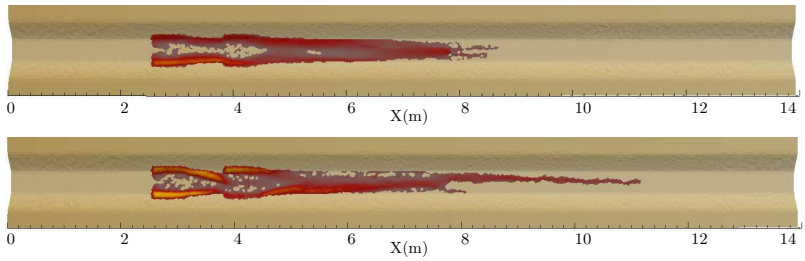

Configuration 4 .

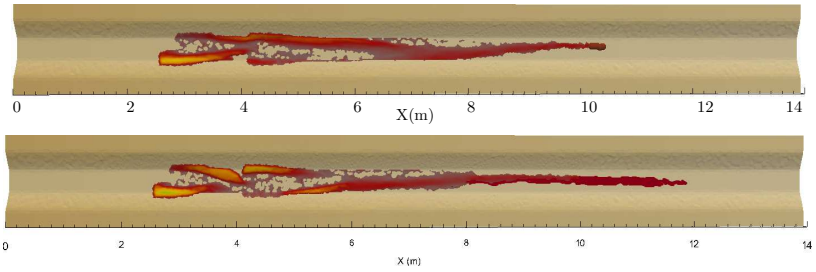

Figure 8: 3D computed contour views of the deposition depth for configurations 3 and 4 at time $t = 30\ min$ with a constant Manning parameter (upper) and with a dynamic Manning parameter (below)

Configuration 1

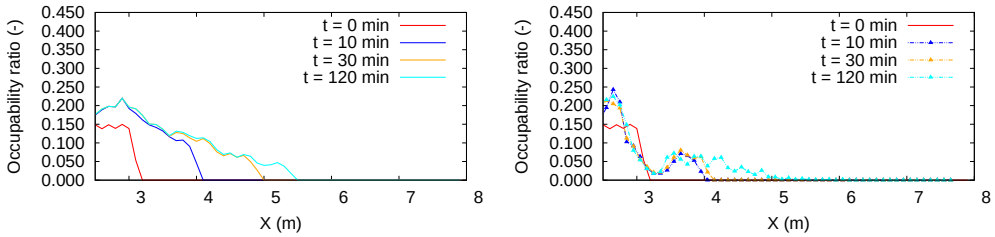

Configuration 2

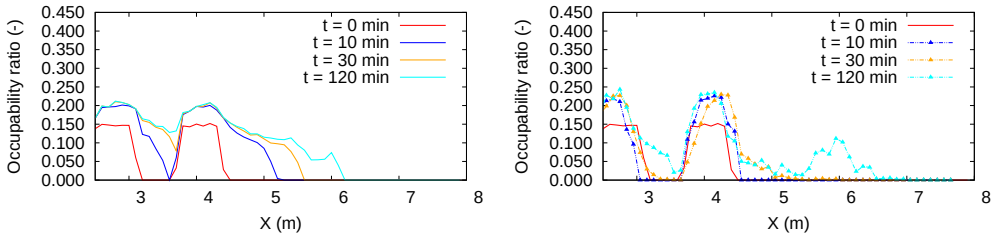

Configuration 3

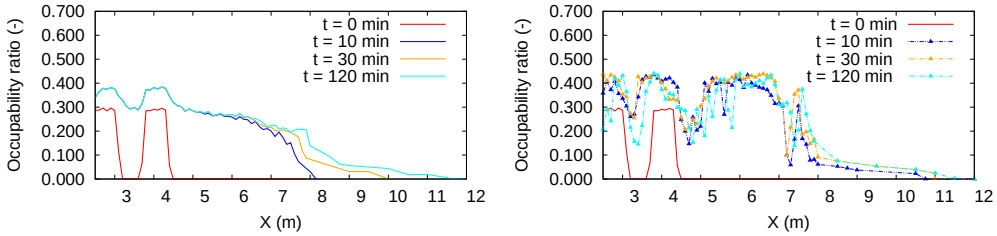

Configuration 4

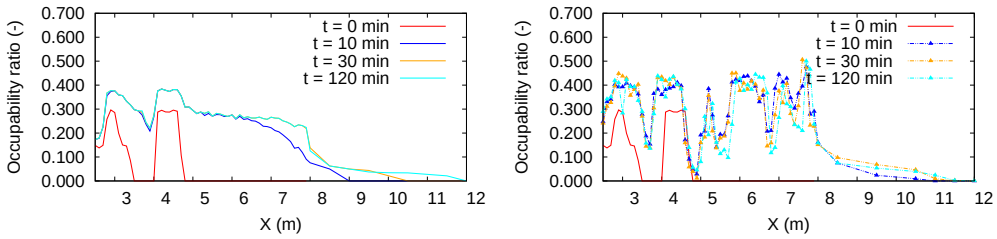

Figure 9: Temporal evolution of the occupability ratio (OR) for the four configurations: numerical results (left) and experimental data (right)

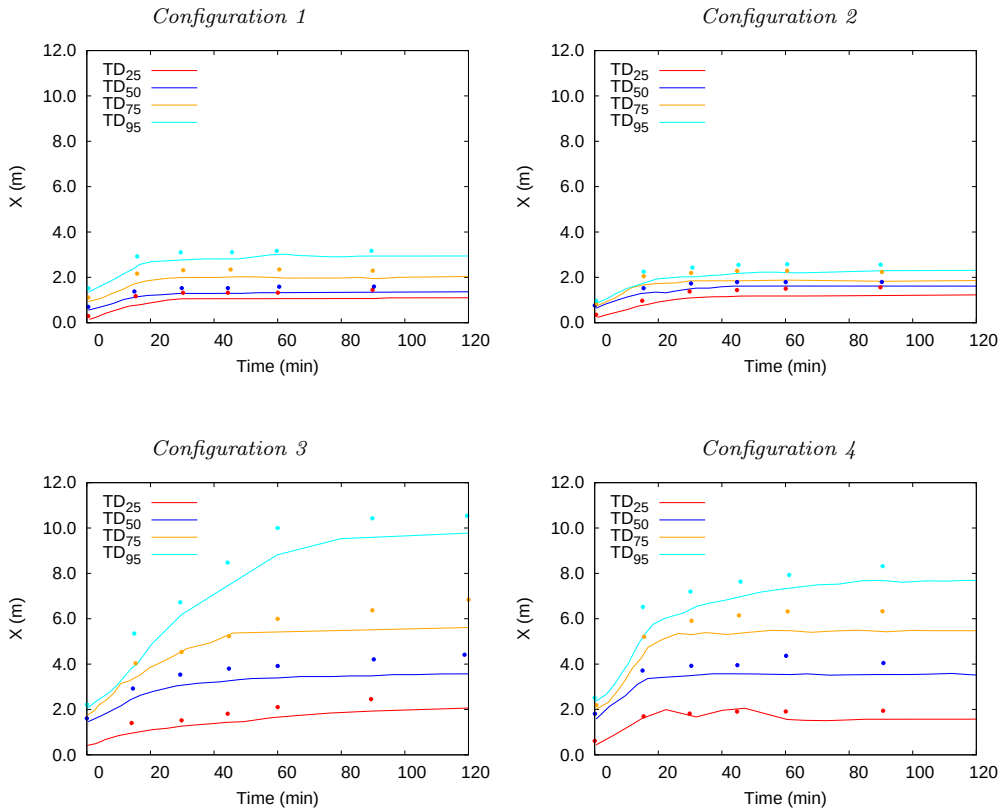

Figure 10: Temporal evolution of the travel distance (TD) for each configuration obtained with numerical simulation (continuous lines) and the experimental data (points)

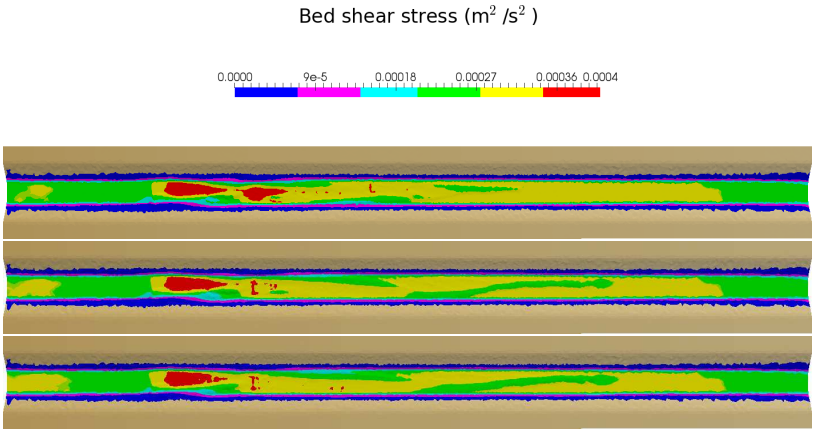

Figure 11: Computed contours of the bed shear stress at times t= 10, 30 and 120 *min* for configuration 4

5. Conclusions

Here, the potential of a numerical tool to assess the success of the application of replenishment of sediment in underfed armored channels is investigated by comparison with empirical data. The effect of several replenishment configurations in the downstream reach were simulated using a 2D Finite Volume scheme able to predict the sediment dynamics in combination with the flow behavior in a self-stable fashion. The mathematical model is built by means of the depth-averaged equations. In addition, the solid and liquid fluxes and source term discretization were derived from an approximate Rienman Problem. The forecasting abilities of the numerical tool when dealing with these environmental present real problems are herein showed and discussed.

Four different replenishment configurations have been studied. The first two configurations are simple but they allow to assess preliminarily the capabilities of the numerical tool. The deposition of the material in the downstream reach which is evaluated in terms of spreading using two parameters, occupational ratio and travel distance, is well tracked.

The third and fourth non-parallel configurations produce more complex deposition patterns and the interaction among blocks drive to a larger spreading. The patterns observed in laboratory are not fully predicted by the simulation. This is justified because in certain areas of the non-erodible channel there is a small number of particles whose transport behavior is mainly governed by collisional forces. The current numerical tool, based on a continuum approach, is still not suitable for this kind of particle-particle interaction. Nevertheless, the main replenishment structures are well captured in time and space by the simulation: maximum run-out, occupational ratio and travel distance.

Furthermore, another important remark is the temporal evolution of the bed roughness due to the new material supply which is provided by the replenishment. It is crucial to distinguish which characteristic grain diameter, between the non-erodible channel bed and the replenishment material, is dominating the bottom friction for obtaining accurate results. The methodology proposed in this work for updating continuously the friction factor leads to suitable results. The above findings show the usefulness of the considered model for the simulation of future different replenishment configurations.

6. Acknowledgments

This work was funded by the ITN-Programme (Marie Curie Actions) of the European Union's Seventh Framework Programme FP7-PEOPLE-2013-ITN under REA grant agreement n_607394-SEDITRANS. The sediment replenishment experiments were funded by FOEN (Federal Office for the Environment, Switzerland).

References

[1] Brandt SA. Classification of geomorphological effects downstream of dams. Catena 2000;40(4):375–401.

[2] Petts GE, Gurnell AM. Dams and geomorphology: Research progress and future directions. Geomorphology 2005;70(1-2):27–47.

[3] Grant GE, Schmidt JC, Lewis SL. A Geological Framework for Interpreting Downstream Effects of Dams on Rivers. Water Science and Application 2005;7):209–225.

[4] Power ME, Dietrich WE, Finlay JC. Dams and Downstream Aquatic Biodiversity: Potential Food Web Consequences of Hydrologic and Geomorphic Change. Environmental Management 1996;20(6):887–895.

[5] Kondolf GM. HungryWater: Effects of Dams and Gravel Mining on River Channels. Environmental Management 1997;21(4):533–551.

[6] Merz JE, Pasternackc GB, Wheaton JM. Sediment budget for salmonid spawning habitat rehabilitation in a regulated river. Geomorphology 2006;76(1-2):207–228.

[7] Kantoush SA, Sumi T, Suzuki T, Murasaki M. Impacts of sediment flushing on channel evolution and morphological processes: Case study of the Kurobe River, Japan. Proc., River Flow 2010 International Conference on Fluvial Hydraulics. 2010.

[8] Balland P. Impacts des barrages sur les milieux physiques et biologiques. Ingénieries: Supplément 2004;38:23–32.

[9] Ock G, Sumi T, Takemon Y. Sediment replenishment to downstream reaches below dams: implementation perspectives. Hydrological Research Letters 2013;7(3):54–59. doi:{doi.org/10.3178/hrl.7.54}.

[10] Venditti JG, Dietrich WE, Nelson PA, Wydzga MA, Fadde J, Sklar L. Effect of sediment pulse grain size on sediment transport rates and bed mobility in gravel bed rivers. Journal of Geophysical Research 2010;115(3):1–19. doi:{10.1029/2009jf001418}.

[11] Zeh M, Donni W. Restoration of spawning grounds for trout and grayling in the river High-Rhine. Aquatic science 1994;56(1):59–69.

[12] Gaeuman D. Mitigating Downstream Effects of Dams. Gravel-Bed Rivers: Processes, Tools, Environments 2012;Unique volume:182–189.

[13] Wheaton JM, Wheatonab JM, Pasternackc GB, Merz JE. Spawning habitat rehabilitation – II. Using hypothesis development and testing in design, Mokelumne River, California, U.S.A. International Journal River Basin Management 2004;2(1):21–37.

[14] Gaeuman D. Recommended quantities and gradation for long-term coarse sediment augmentation downstream from Lewiston Dam. 2008.

[15] Sklar LS, Fadde J, Venditti JG, Nelson P, Wydzga MA, Cui Y, et al. Translation and dispersion of sediment pulses in flume experiments simulating gravel augmentation below dams. Water Resources Research 2009;45(8):n/a. doi:{10.1029/2008WR007346}.

[16] Lisle TE, Pizzuto JE, Ikeda H, Iseya F, Kodama Y. Evolution of a sediment wave in an experimental channel. Water Resources Research 1997;8:1971–1981.

[17] Cui Y, Parker G, Pizzuto JE, Lisle TE. Sediment pulses in mountain rivers: 1. Comparison between experiments and numerical predictions. Water Resources Research 2003;39(9):1240. doi:10.1029/2002WR001805.

[18] Ikeda H. Experiments on bedload transport,bed forms,and sedimentary structures using fine gravel in the 4-meter-wide flume. Environmental Research Center papers 1983;2:1–78.

[19] Venditti JG, Nelson P, Minear JT, Wooster J, Dietrich WE. Alternate bar response to sediment supply termination. Journal of Geophysical Research 2012;117(2):1–18. doi:{10.1029/2011jf002254}.

[20] Nelson PA, Brew AK, Morgan JA. Morphodynamic response of a variable-width channel to changes in sediment supply. Water Resources Research 2015;accepted:n/a. doi:{10.1002/2014WR016806}.

[21] Gaeuman D. High-Flow Gravel Injection for Constructing Designed in-Channel Features. River Research and Applications 2014;30(6):685–706. doi:{10.1002/rra.2662}.

[22] Gomez B, Church M. An assessment of bed load sediment transport formulae for gravel bed rivers. Water Resources Research 1989;25(6):1161–1186. doi:{10.1029/WR025i006p01161}.

[23] Aricò C, Tucciarelli T. Diffusive Modeling of Aggradation and Degradation in Artificial Channels. Journal of Hydraulic Engineering 2008;134(8):1079–1088. doi:{10.1061/(ASCE)0733-9429(2008)134:8(1079)}.

[24] Wu W. Depth-Averaged Two-Dimensional Numerical Modeling of Unsteady Flow and Nonuniform Sediment Transport in Open Channels. Journal of Hydraulic Engineering 2004;130(10):1013–1024.

[25] Soares-Frazao S, Zech Y. HLLC scheme with novel wave-speed estimators appropiate for two-dimensional shallow-water flow on erodible bed. International Journal of Numerical Methods in Fluids 2010;66(8):1019–1036. doi:{10.1080/00221686.2012.689682}.

[26] Siviglia A, Stecca G, Vanzo D, Zolezzi G, Toro E, Tubino M. Numerical modelling of two-dimensional morphodynamics with applications to river bars and bifurcations. Advances in Water Resources 2013;52:243–260. doi:{dx.doi.org/10.1016/j.advwatres.2012.11.010}.

[27] Canelas R, Murillo J, Ferreira RML. Two-dimensional depth-averaged modelling of dambreak flows over mobile beds. Journal of Hydraulic Research 2013;51(4):392–407. doi:{10.1080/00221686.2013.798891}.

[28] Villaret C, Hervouet J, Kopmann R, Merkel U, Davies A. Morphodynamic modeling using the Telemac finite-element system. Computers and Geosciences 2013;53:105–113. doi:{10.1016/j.cageo.2011.10.004}.

[29] Liu X, Landry B, García M. A hybrid Lattice Boltzmann method-finite difference method model for sediment transport and riverbed deformation. River Research and Applications 2015;31:447–456. doi:{10.1002/rra.2735}.

[30] Juez C, Murillo J, García-Navarro P. A 2D weakly-coupled and efficient numerical model for transient shallow flow and movable bed. Advances in Water Resources 2014;71:93–109. doi:{10.1016/j.advwatres.2014.05.014}.

[31] Battisacco E, Franca MJ, Schleiss AJ. Physical modeling of artificial river replenishment techniques to restore morphological conditions downstream of dams. Proceeding IAHR 2015 World Congress. ????

[32] Murillo J, García-Navarro P. Weak solutions for partial differential equations with source terms: Application to the shallow water equations. Journal of Computational Physics 2010;229:4327–4368. doi:{10.1016/j.jcp.2010.02.016}.

[33] Juez C, Murillo J, García-Navarro P. Numerical assesment of bed load discharge formulations for transient flow in 1D and 2D situations. Journal of Hydroinformatics 2013;15(4):1234–1257. doi:{10.2166/hydro.2013.153}.

[34] Smart G. Sediment transport formula for steep channels. Journal of Hydraulic Engineering 1984;3:267–276.

[35] Ferreira RML, Franca MJ, Leal JGAB, Cardoso AH. Flow over rough mobile beds: Friction factor and vertical distribution of the longitudinal mean velocity. Water Resources Research 2012;48:W05529. doi:{10.1029/2011WR011126}.

[36] Ferreira RML. The von Kármán constant for flows over rough mobile beds. Lessons learned from dimensional analysis and similarity. Advances in Water Resources 2015;81:19–32. doi:{10.1016/j.advwatres.2014.10.004}.

[37] Manning R. On the flow of water in open channels and pipes. Transactions of the Institution of Civil Engineers of Ireland 1895;20:161–207.

[38] Strickler A. Beiträge zur Frage der Geschwindigheitsformel und der Rauhigkeitszahlen für Ströme, Kanale und geschlossene Leitungen. Mitteilungen des Eidgenössischen Amtes für Wasserwirtschaft 1923;:16 pp.

[39] Ferguson R, Hoey T, Wathen S, Werrity A. Field evidence for rapid downstream fining of river gravels through selective transport. Geology 1996;24(2):179–182.

[40] Hoey T, Bluck BJ. Identifying the controls over downstream fining of river gravels. Journal of Sedimentary Research 1999;69(1):40–50.

[41] Frings RM. Downstream fining in large sand-bed rivers. Earth Science Reviews 2008;87:39–60.

[42] Wright S, Parker G. Modeling downstream fining in sand-bed rivers I: Formulation. Journal of Hydraulic Research 2005;43(6):612–619.

[43] Wright S, Parker G. Modeling downstream fining in sand-bed rivers I: Application. Journal of Hydraulic Research 2005;43(6):620–630.

[44] Manning M. Development of channel organization and roughness following sediment pulses in single-thread, gravel bed rivers. Water Resources Research 2001;37(8):2259–2272.

[45] Ferguson RI, Church M, Rennie CD, Venditti JG. Reconstructing a sediment pulse: Modeling the effect of placer mining on Fraser River, Canada. Journal of Geophysical Research: Earth Surface 2015;120:1436–1454. doi:{10.1002/2015JF003491}.